Article ID: 1006-3471(2006)03-0250-07

Investigations on Electrochemical Characteristics of LiV_3O_8 Electrode in Lithium Sulfate-water-ethanol Electrolytes

YUAN An-bao*, SONG Wei-xiang
(Department of Chemistry, College of Sciences, Shanghai University, Shanghai 200444, China)

Abstract: The active material of LiV_3O_8 prepared using low-temperature pre-reaction in solution followed by intermediate-temperature calcination at 450 ℃. The product was characterized by X-ray diffraction analysis and scanning electron microscope observation. The performance of LiV_3O_8 electrode in neutral lithium sulfate-water-ethanol electrolytes was investigated using electrochemical methods. Galvanostatic charge/discharge results indicated that the specific capacity of LiV_3O_8 electrode decreases with ethanol content increasing in electrolyte. The most appropriate water/ethanol volumetric ratio is 4∶1 in terms of conductivity of the electrolyte and stability of the electrode. AC impedance measurements demonstrated that the ohmic resistance of the electrolyte as well as the charge transfer resistance of the electrode/electrolyte interface increases with ethanol content increasing.

Key words: Lithium trivanadate, Electrochemical characteristics, Lithium sulfate-water-ethanol lectrolyte
CLC Number: TM 912 **Document Code:** A

1 Introduction

Lithium ion batteries have been applied to many fields such as communication, portable computer and so on, owing to the advantages of high specific energy, long cycle life and environmentally friendship. However, there are some disadvantages with nonaqueous lithium ion batteries such as safety problem in utilization, high manufacturing cost and low conductivity of organic electrolyte. These drawbacks limited its application to some areas, for example, in application to electric vehicles.

From 1994, studies on lithium ion batteries or Li^+ insertion/extraction electrode materials using aqueous electrolyte containing lithium ions were reported[1-8]. Lithium trivanadate, LiV_3O_8 ($Li_{1+x}V_3O_8$) have been intensively investigated as positive electrode materials in nonaqueous lithium batteries[9-17]. It is well known that the Li^+ insertion/extraction potential of LiV_3O_8 is lower than that of $LiCoO_2$ and $LiNiO_2$. Hence, J. Köhler *et al*[8] studied the battery with LiV_3O_8 ($Li_{1+x}V_3O_8$) as negative electrode, $LiNi_{0.81}Co_{0.19}O_2$ as positive electrode and 1 mol/L Li_2SO_4 aqueous solution as electrolyte. Wherein, the LiV_3O_8 crystal was prepared by conventional high-temperature solid method. In our previous work[18], the LiV_3O_8 material was prepared using low-temperature solution reaction followed by intermediate-temperature calcination method (ascribed to solution method) and its electrochemical performance as negative electrode in 1 mol/L Li_2SO_4 aqueous electrolyte was examined. We found that the charge/discharge capacity of the solution-method LiV_3O_8 was higher than that of the solid-method one. Nevertheless, the capacity degradation of the LiV_3O_8 electrode upon cycling was still quick

Received date: 2005-11-24 * Corresponding author, Tel: (86-21) 66134851, E-mail: abyuan@staff.shu.edu.cn

due to the aqueous electrolyte. Alternatively, in the present study, lithium sulfate-water-ethanol solution electrolytes were employed and the influence of different water/ethanol volumetric ratios on the electrochemical performance of LiV_3O_8 electrode was investigated.

2 Experimental

2.1 Preparation of LiV_3O_8 Material

The LiV_3O_8 material was prepared according to the method described in literature[13]. Li_2CO_3 and NH_4VO_3 (analytical grade) with a molar ratio of Li∶V = 1∶3 were added to distilled water in a beaker, then heated to boiling with magnetic stirring. Boiling for about 1 h, the solids were thoroughly dissolved. After boiling off the water completely, a solid mixture (precursor) was produced. The precursor was heated to 450 ℃ and maintained for 10 h (calcination) in an electric furnace and cooled down to room temperature, thus the LiV_3O_8 material was obtained.

2.2 Thermal Analysis, Structure Characterization and Morphology Observation

Thermogravimetric and differential thermal analysis (TG-DTA) of the precursor (pre-reaction product) was performed using a microcomputer controlled WCT-1A differential thermal analysis unit (Beijing, China). The temperature rise rate was controlled at 10 ℃·min^{-1} heating from 26 to 500 ℃, and the mass of the sample was about 10 mg. The crystal structure of LiV_3O_8 active material was characterized by powder X-ray diffraction (XRD) analysis using a Rigaku D/max-RB X-ray diffractometer with CuK_α radiation (40 kV/40 mA). Morphology observations of the LiV_3O_8 product and the precursor were conducted on a Hitachi S-350 scanning electron microscope (SEM).

2.3 Preparation of LiV_3O_8 Electrodes

A given amount of LiV_3O_8 and 10% (by mass) acetylene black were mixed, then 5% poly(tetrafluoroethylene) emulsion was added to the mixture and mixed thoroughly again. The obtained paste was filled into foamed nickel with 2 cm × 2 cm dimensions. The pasted electrode was dried at 70 ℃ for 12 h and then roll-pressured to a thickness of 0.6 mm.

2.4 Electrochemical Testing

Charge/discharge performance of LiV_3O_8 electrodes was performed using LAND auto-cycler (China). The working electrode was LiV_3O_8 electrode, the counter electrode was $LiNiO_2$ electrode with higher capacity relatively, and the reference electrode was saturated calomel electrode (SCE). 2 mol/L Li_2SO_4-water-ethanol solutions were used as electrolytes. The charge and discharge cut off potentials were -1.5 and -0.2 V (vs SCE) respectively.

Electrochemical impedance spectroscopy (EIS) of LiV_3O_8 electrodes were carried out using CHI660A Electrochemical Work Station with the three-electrode system same as the above.

3 Results and Discussion

3.1 TG-DTA Curves of the Precursor and the Preparation Reaction

The pre-reaction in solution can be described by the following equation[13]:

$$6NH_4VO_3 + Li_2CO_3 \longrightarrow 2NH_4V_3O_8 \cdot xH_2O + Li_2CO_3 + 4NH_3 + 2(1-x)H_2O \quad (1)$$

In Eq. (1), NH_4VO_3 changed to $NH_4V_3O_8 \cdot xH_2O$ and in the meanwhile, NH_3 and H_2O were given off. Whereas, Li_2CO_3 underwent no net change in the reaction, but its presence in this process helped to form homogeneous mixture (precursor) and would be convenient for the solid reaction in the subsequent calcination process:

$$2NH_4V_3O_8 \cdot xH_2O + Li_2CO_3 \longrightarrow 2LiV_3O_8 \cdot yH_2O + 2NH_3 + CO_2 + (1+2x-2y)H_2O \quad (2)$$

$$LiV_3O_8 \cdot yH_2O \longrightarrow LiV_3O_8 + yH_2O \quad (3)$$

The thermograms of the precursor are shown in Fig. 1. Wherein the first mass loss before 150 ℃ is due to the dehydration of free water in the mixture. The second weight loss in the range of 150～230 ℃ with the DTA peak at 190 ℃ should be ascribed to the escape of NH_3, CO_2 and H_2O[13] which corresponding to the reaction (2). The third weight loss between 230～320 ℃ should be attributed to the re-

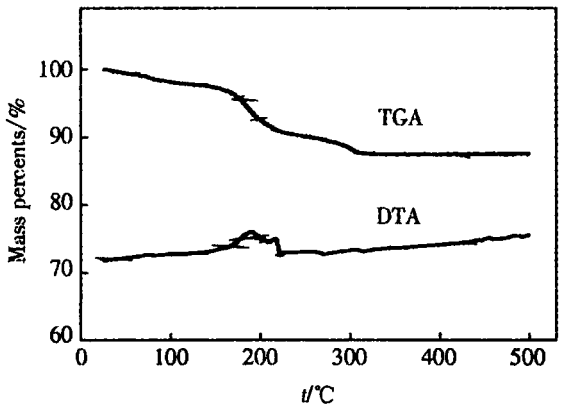

Fig 1 TG-DTA curves of the precursor

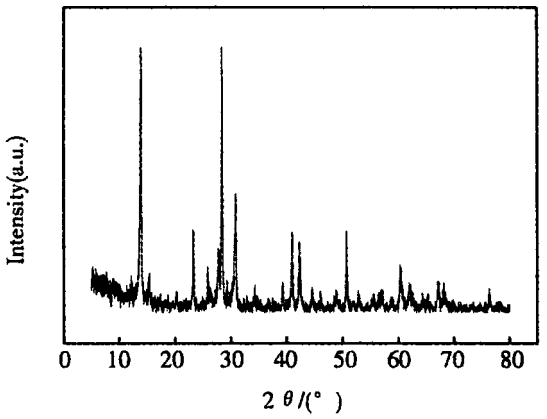

Fig 2 XRD pattern of the LiV_3O_8 powders

moval of the intercalated water in $LiV_3O_8 \cdot yH_2O$ interlayer. This process corresponds to the equation (3). The residual water in V_3O_8 layer could be removed completely after 320 ℃. In this study, a temperature of 450 ℃ was selected as calcination temperature for the LiV_3O_8 preparation.

3.2 XRD Analysis and SEM Observation

Fig 2 shows the powder X-ray diffraction pattern of the LiV_3O_8. It can be seen from Fig 2 that the characteristic peaks for LiV_3O_8 are presented in 2θ = 13.92°, 23.28°, 28.36°, 30.86°, 41.04°, 42.30° and 50.70° respectively. This suggests that the prepared LiV_3O_8 is a pure single-phase compound.

The SEM images of the precursor and the LiV_3O_8 product are shown in Fig 3a and b respectively. The precursor exhibits polycrystalline aggregation of the mixture. While, the LiV_3O_8 crystal presents wide particle size distribution.

3.3 Charge/Discharge Characteristics and AC Impedance Spectra Analysis of the LiV_3O_8 Electrode

Fig 4 shows the first charge/discharge curves of the LiV_3O_8 electrode in 2 mol/L Li_2SO_4-water-ethanol electrolytes with different water/ethanol volumetric ratios. On charging process, the Li^+ ions in solution are intercalated to $Li_{1+x}V_3O_8$ and the electrode potential decreases. While on discharging, the Li^+ ions in $Li_{1+x}V_3O_8$ are deintercalated to solution and the electrode potential increases. With ethanol content in-

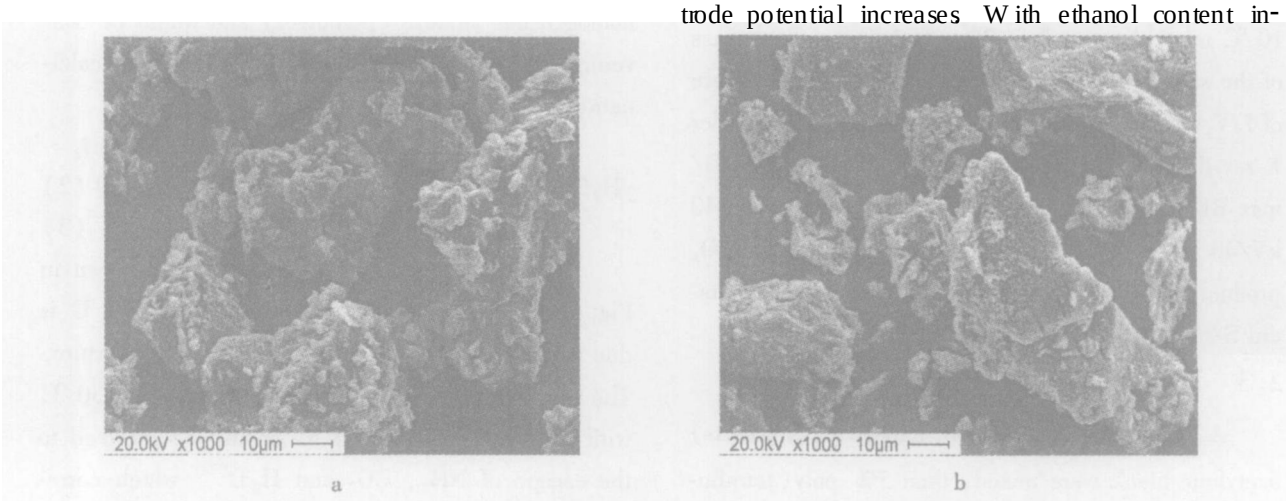

Fig 3 SEM images of the precursor (a) and the LiV_3O_8 (b)

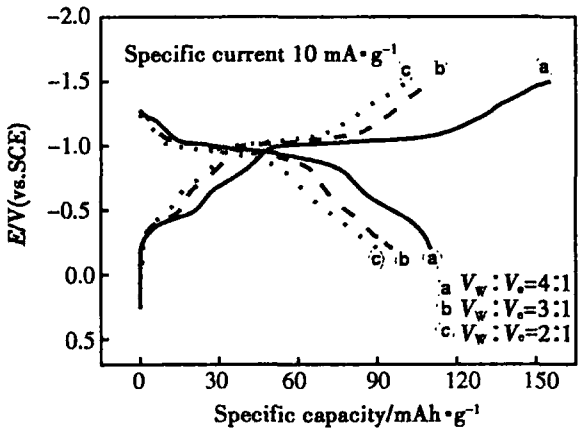

Fig 4　First charge/discharge curves of the LiV_3O_8 electrode in 2 mol/L Li_2SO_4-water-ethanol electrolytes with different water/ethanol volumetric ratios

creasing in electrolyte, the average charge potential decreases and the average discharge potential increases. The maximal charge/discharge specific capacity was obtained with a water/ethanol volumetric ratio of 4∶1. Nevertheless, we found from experiment that if the ethanol content decreases further, the electrode would become unstable in the electrolyte. Hence, the water/ethanol volumetric ratio of 4∶1 is considered to be the most appropriate for simultaneously considering the conductivity of the electrolyte (see below) and the stability of the electrode.

To correlate the above charge/discharge results with AC impedance behavior, the AC impedance spectra for the LiV_3O_8 electrode in 2 mol/L Li_2SO_4-water-ethanol electrolytes with different water/ethanol volumetric ratios were obtained and displayed in Fig 5. Before AC impedance measurements, the electrode had gone through an initial charge/discharge cycle for activation. The AC impedance were measured at discharged state (i.e. 0% SOC, State Of Charge) with the frequency range from 10^5 to 10^{-3} Hz. Fig 5b is the close up view of Fig 5a at high frequency region. Seen from Fig 5a that the impedance spectra are all composed of a semicircle and a straight line. The semicircle at the higher frequency region should be attributed to the charge transfer resistance of the electrode/electrolyte interface, and the straight line at the lower frequency region corresponds to the Warburg diffusion impedance of Li^+ in solid. The charge transfer resistance increases with ethanol content increasing in electrolyte. On the other hand, seen from Fig 5b that the ohmic resistance increases with ethanol content increasing in electrolyte. This is because that the conductivity of the solution decreases with ethanol content increasing. Therefore, it comes to the conclusion that with ethanol content increasing in electrolyte, not only ohmic resistance of the electrolyte, but also the charge transfer resistance of the electrode/electrolyte interface are increased.

Fig 6 shows the charge/discharge curves of the LiV_3O_8 electrode at different specific currents in 2 mol/L Li_2SO_4-water-ethanol-electrolyte. With charge/discharge specific currents increasing, the average charge potential and the average discharge potential shift toward more negative and more positive respectively, and hence the charge/discharge capacity decreases. The capacity at specific current of 20 mA·g^{-1} decreased not significantly compared with that at 10 mA·g^{-1}, but the capacity at 30 or 50 mA·g^{-1}

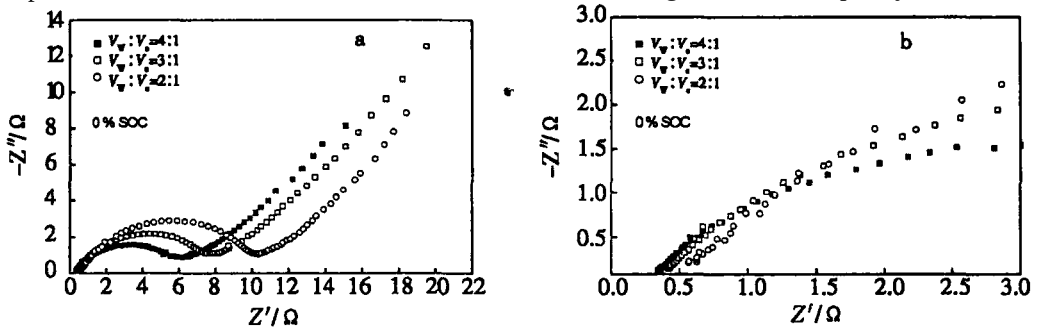

Fig 5　AC impedance spectra for the LiV_3O_8 electrode in 2 mol/L Li_2SO_4-water-ethanol electrolytes with different water/ethanol volumetric ratios

decreased obviously.

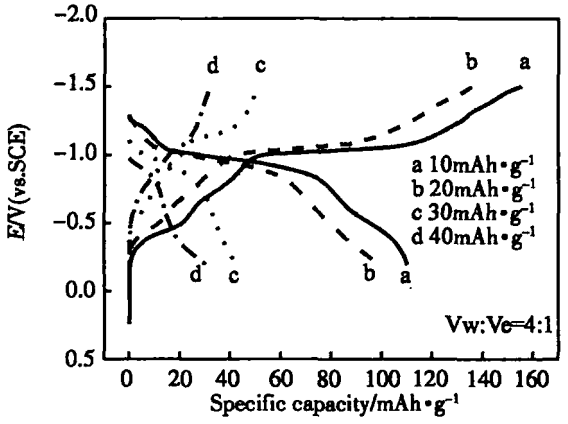

Fig 6 Charge/discharge curves of the LiV_3O_8 electrode at different specific currents in 2 mol/L Li_2SO_4-water-ethanol electrolyte

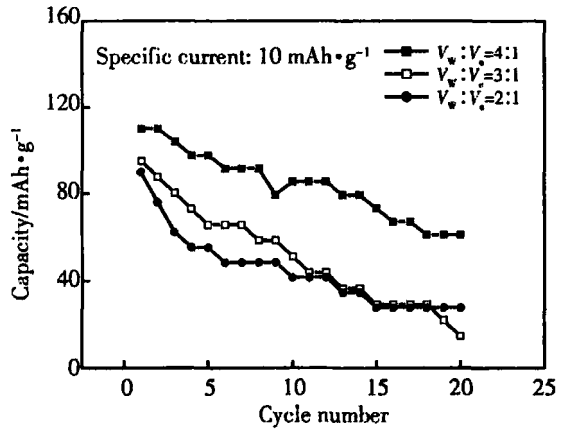

Fig 7 Variation of Discharge capacity with cycle number for the LiV_3O_8 electrode cycled in 2 mol/L Li_2SO_4-water-ethanol electrolytes with different water/ethanol volumetric ratios

The charge / discharge cyclic stability of the LiV_3O_8 electrode at a specific current of 10 mA · g^{-1} in 2 mol/L Li_2SO_4-water-ethanol electrolytes with different water/ethanol ratios are presented in Fig 7. Seen from Fig 7, that the specific discharge capacity of the electrode in the electrolyte with water/ethanol ratio of 4 ∶1 is obviously higher than that in the electrolyte with water/ethanol ratio of 3 ∶1 or 2 ∶1. Moreover, in the initial 5 cycles, the capacity decline rate of the electrode in the electrolyte with water/ethanol ratio of 4 ∶1 is slower than that in the other electrolytes. Undergone 20 charge/discharge cycles, the discharge capacity of the electrode in the electrolyte with water/ethanol ratio of 4 ∶1 decreased to 61 % of the initial value. Although the capacity degradation with cycling is still quick, the cyclic stability is improved in some degree compared to the LiV_3O_8 electrode cycled in lithium sulfate-water aqueous electrolyte[18].

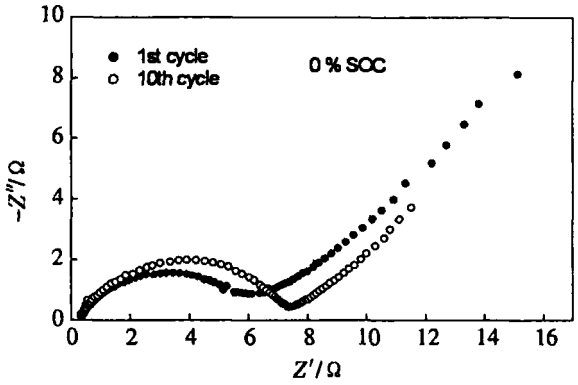

Fig 8 AC impedance spectra of the LiV_3O_8 electrode being cycled 1 and 10 cycles in 2 mol/L Li_2SO_4-water-ethanol electrolyte

Fig 8 shows the AC impedance spectra of the LiV_3O_8 electrode being cycled 1 and 10 cycles at specific current of 10 mA · g^{-1} in 2 mol/L Li_2SO_4-water-ethanol electrolyte with water/ethanol ratio of 4 ∶1. The AC impedance measurements were performed at discharged state (0% SOC) and with the frequency range from 10^5 to 10^{-3} Hz. Seen from Fig 8 that undergone 10 charge/discharge cycles, the semicircle at higher frequency region increased obviously. This indicates that upon cycling, the charge transfer resistance of the electrode/electrolyte interface increased and the electrochemical reactivity of the electrode decreased.

4 Conclusions

The LiV_3O_8 electrode can intercalate and deintercalate Li^+ ions in lithium sulfate-water-ethanol electrolyte and may be used as negative electrode for lithium ion battery with aqueous electrolyte. The galvanostatic charge/discharge results demonstrated that the charge/discharge specific capacity of the LiV_3O_8 electrode decreased with ethanol content increasing in

electrolyte. A maximal specific discharge capacity of 110 mAh·g^{-1} was obtained in the electrolyte with water/ethanol volumetric ratio of 4∶1, and this composition is considered to be the most appropriate for simultaneously considering the conductivity and stability. AC impedance results revealed that with ethanol content increasing in electrolyte, not only ohmic resistance of the electrolyte, but also the charge transfer resistance of the electrode/electrolyte interface increased. Cyclic stability investigation showed that undergone 20 charge/discharge cycles, the discharge capacity of the LiV_3O_8 electrode in the electrolyte with water/ethanol volumetric ratio of 4∶1 decreased to 61% of the initial value. The charge transfer resistance of the electrode/electrolyte interface was increased upon cycling and this reflects the decreasing of electrochemical reactivity of the electrode.

References:

[1] Li Wu, Dahn J R, Wainwright D S. Rechargeable lithium batteries with aqueous electrolytes[J]. Science, 1994, 264: 1115～1118.

[2] Li Wu, McKinnon W R, Dahn J R. Lithium intercalation from aqueous solutions[J]. J. Electrochem. Soc., 1994, 141(9): 2310～2315.

[3] Li Wu, Dahn J R. Lithium-ion cells with aqueous electrolytes[J]. J. Electrochem. Soc., 1995, 142(6): 1742～1745.

[4] Zhang Mei-jie, Dahn J R. Electrochemical lithium intercalation in VO_2(B) in aqueous electrolytes[J]. J. Electrochem. Soc., 1996, 143(9): 2730～2735.

[5] Yang H Q, Li D P, Han S, et al. Vanadium-manganese complex oxides as cathode materials for aqueous solution secondary batteries[J]. J. Power Sources, 1996, 58: 221～224.

[6] Yang Hui, Yang Hua-quan, Lu Yin-lin, et al. Research of Zn-Mn spinel electrode mateial for aqueous secondary batteries[J]. J. Power Sources, 1996, 62: 223～227.

[7] Wang Pei, Yang Hui, Yang Hua-quan. Electrochemical behavior of Li-Mn spinel electrode mateial in aqueous solution[J]. J. Power Sources, 1996, 63: 275～278.

[8] Köhler J, Makihara H, Uegaito H, et al. LiV_3O_8: Characterization as anode material for an aqueous rechargeable Li-ion battery system[J]. Electrochim. Acta, 2000, 46: 59～65.

[9] Panero S, Pasquali M, Pistoia G. Rechargeable Li/$Li_{1+x}V_3O_8$ cells[J]. J. Electrochem. Soc., 1983, 130(5): 1225～1227.

[10] Pistoia G, Pasquali M, Wang G, et al. $Li/Li_{1+x}V_3O_8$ secondary batteries: synthesis and characterization of an amorphous form of the cathode[J]. J. Electrochem. Soc., 1990, 137(8): 2365～2370.

[11] West K, Zachau-Christiansen B, Skaarup S, et al. Comparison of LiV_3O_8 cathode materials prepared by different methods[J]. J. Electrochem. Soc., 1996, 143(3): 820～825.

[12] Kumagai N, Yu A. Ultrasonically treated LiV_3O_8 as a cathode material for secondary lithium batteries[J]. J. Electrochem. Soc., 1997, 144(3): 830～834.

[13] Dai Jin-xiang, Sam F Y L, Gao Zhi-qiang, et al. Low-temperature synthesized LiV_3O_8 as a cathode material for rechargeable lithum batteries[J]. J. Electrochem. Soc., 1998, 145(9): 3057～3062.

[14] Kawakita J, Miura T, Kishi T. Charging characteristics of $Li_{1+x}V_3O_8$[J]. Solid State Ionics, 1999, 118: 141～147.

[15] Liu G Q, Zeng C L, Yang K. Study on the synthesis and properties of LiV_3O_8 rechargeable lithium batteries cathode[J]. Electrochim. Acta, 2002, 47: 3239～3243.

[16] Xie Jing-gang, Li Jin-xia, Zhan Hui, et al. Low-temperature sol-gel synthesis of $Li_{1.2}V_3O_8$ from V_2O_5 gel[J]. Mater. Lett., 2003, 57: 2682～2687.

[17] Xu Hai-yan, Wang Hao, Song Zhi-qiang, et al. Novel chemical methode for synthesis of LiV_3O_8 nanorods as cathode materials for lithium ion batteries[J]. Electrochim. Acta, 2004, 49: 349～353.

[18] Song Wei-xiang, Yuan An-bao, Zhao Jun. Electrochemical properties of LiV_3O_8 prepared by solution method[J]. Battery Bimonthly, 2005, 35(2): 91～92.

LiV_3O_8电极在硫酸锂-水-乙醇电解质中的电化学性能研究

袁安保*，宋维相
(上海大学理学院化学系，上海 200444)

摘要： 应用低温液相反应再经450℃中温锻烧制备LiV_3O_8活性物质，并用X射线衍射(XRD)分析和扫描电镜(SEM)表征了产物LiV_3O_8结构、形貌. 电化学方法研究LiV_3O_8电极在硫酸锂-水-乙醇中性电解质溶液中的性能. 恒流充放电结果表明，LiV_3O_8电极的比容量随电解质溶液中乙醇含量的增加而降低，若同时考虑电解质溶液的电导率和电极的稳定性，水/乙醇体积比4∶1最为合适. 交流阻抗测试表明，溶液的欧姆电阻以及电极/电解质界面的电荷转移电阻随溶液中乙醇含量的增加而增大；随着充放电循环的进行，电极/电解质界面的电荷转移电阻增大，电极的活性降低.

关键词： LiV_3O_8；电化学特性；硫酸锂-水-乙醇电解质